

Processing and Piezoelectric Properties of $(\text{Na}_{0.5}\text{K}_{0.5})_{0.96}\text{Li}_{0.04}(\text{Ta}_{0.1}\text{Nb}_{0.9})_{1-x}\text{Cu}_x\text{O}_{3-3x/2}$ Lead-Free Ceramics

Ruzhong Zuo,[†] Chun Ye, and Xusheng Fang

School of Materials Science and Engineering, Hefei University of Technology, Hefei 230009, China

Zhenxing Yue and Longtu Li*

State Key Lab of New Ceramics and Fine Processing, Department of Materials Science and Engineering, Tsinghua University, Beijing 100084, China

The Cu-modified $(\text{Na}_{0.5}\text{K}_{0.5})_{0.96}\text{Li}_{0.04}\text{Ta}_{0.1}\text{Nb}_{0.9}\text{O}_3$ lead-free piezoelectric ceramics were fabricated at relatively low temperatures by ordinary sintering. The results indicate that the addition of copper oxide (CuO) does not change the crystal structure and the dielectric–temperature characteristic, but tends to slightly increase the loss tangent and significantly modify the ferroelectric and electromechanical properties. Moreover, the grains get clearly coarsened with increasing CuO content. When doped with <0.25% CuO, the materials get softer with slightly decreased coercive fields (E_c) and increased maximum electric field-driven strains (S_m), and thus own enhanced piezoelectric properties; however, as the doping level becomes higher, the materials get harder, possessing larger E_c and reduced remanent polarization and S_m . The change in the electrical properties can be attributed to both the formation of oxygen vacancies by Cu^{2+} replacing Nb^{5+} and the modification of densification.

I. Introduction

RESEARCH on lead-free ferroelectric and piezoelectric ceramics or crystals has been more and more concentrated in the last few years, based on concerns about lead pollution from conventional piezoelectric materials, such as $\text{Pb}(\text{Zr,Ti})\text{O}_3$ (PZT). The focus of these studies currently is to search for high-performance lead-free candidate materials with so-called morphotropic phase boundaries (MPB) where it is believed that the materials show superior dielectric, ferroelectric, piezoelectric, and electromechanical properties.^{1–3} So far, two main systems have been investigated for lead-free piezoelectric applications: $(\text{Bi}_{0.5}\text{Na}_{0.5})\text{TiO}_3$ (BNT) and $(\text{Na}_x\text{K}_{0.5})\text{NbO}_3$ (NKN)-based compositions. Compared with BNT-based MPB compositions,^{4–8} NKN-based compositions show many advantages such as higher Curie temperature and better piezoelectric and electromechanical properties, particularly the Li-, Ta-, and Sb-modified NKN compositions.^{9–13} A few systems can be produced, depending on the ratio of Li to Ta or Sb in the final compositions with varying electrical properties and Curie temperatures. These systems look very promising for potential lead-free piezoelectric applications to replace PZT materials. However, these systems also show some disadvantages in some cases, such as abnormal grain growth, poor durability against water, low fatigue resistance, and low stability of piezoelectric properties, etc.^{14,15} Therefore, a number of works have concentrated

on these systems. To our knowledge, the MPB in these systems should attract more attention because it is different from those in conventional Pb-based piezoelectric compositions, such as PZT. It was reported that alkaline niobate solid solution systems have MPBs between perovskite phases and the lithium niobate phases. From the viewpoint of crystal symmetry, it lies between orthorhombic and tetragonal ferroelectric phases.¹⁰ Moreover, a lot of attempts are being made to further improve the properties of currently known systems by different processing routes, for example, powder preparation, doping, shaping, and sintering methods.^{16–22} The use of dopants can usually be expected to expand possible application of the materials by introducing special properties, for example, soft or hard properties in a piezoelectric material for various applications. The purpose of this work is to modify $(\text{Na}_{0.5}\text{K}_{0.5})_{0.96}\text{Li}_{0.04}\text{Ta}_{0.1}\text{Nb}_{0.9}\text{O}_3$ (NKLTN) ceramics by doping a small amount of copper oxide (CuO). Cu ions are anticipated to enter into the B site, generating oxygen vacancies. NKLTN is an MPB-near composition among NKN, LiNbO_3 , and LiTaO_3 , having good electrical properties.⁹ The influence of CuO addition on the crystal structure, microstructure, and various electrical properties are discussed in detail.

II. Experimental Procedure

Ceramics with compositions of $(\text{Na}_{0.5}\text{K}_{0.5})_{0.96}\text{Li}_{0.04}(\text{Ta}_{0.1}\text{Nb}_{0.9})_{1-x}\text{Cu}_x\text{O}_{3-3x/2}$ ($x = 0, 0.0025, 0.005, 0.01, 0.02,$ and 0.04) were synthesized by traditional solid-state sintering. Oxygen vacancies were considered as the charge equilibrium mechanism. The raw materials used in this study were potassium carbonate (K_2CO_3 , 99.5%), sodium carbonate (Na_2CO_3 , 99.5%), lithium carbonate (Li_2CO_3 , 99.5%), tantalum oxide (Ta_2O_5 , 99.0%), copper oxide (CuO, 99.5%), and niobium oxide (Nb_2O_5 , 99.5%). Before weighing, all powders were handled by a special dry process as described previously.¹³ The weighed powders were mixed in a nylon jar with ZrO_2 balls in anhydrous ethanol for 18 h and then calcined at 850°C for 6 h after drying. Before compaction, the calcined powder was milled again for 24 h to improve the sintering activity. Specimens with a thickness of ~ 2 mm and a diameter of ~ 15 mm were pressed in a stainless die under ~ 50 MPa. Sintering was carried out in air in the temperature range of 1050 – 1120°C for 2–5 h. During sintering, the sample was buried in the powder of the same composition and covered with an inverted crucible to minimize the volatilization of lithium and potassium.

Densities of the specimens sintered at different temperatures were measured by the Archimedes method. The microstructure was observed by scanning electron microscopy (JEOL6301F, Tokyo, Japan). Powder X-ray diffraction (Rigaku, Tokyo, Japan) patterns of crushed pellets using $\text{CuK}\alpha$ radiation were recorded in the 2θ range of 20° – 60° .

Silver paste was fired on two major surfaces of each specimen as electrodes after a careful polishing process. Dielectric prop-

D. D. Viehland—contributing editor

Manuscript No. 23556. Received August 6, 2007; approved October 18, 2007.

This work was financially supported by HFUT RenCai Foundation (No. 103-035006) and a special Program for Excellence Selection “R & D of Novel Lead Free Piezoelectric Ceramics” (No. 103-035034).

*Member, the American Ceramic Society.

[†]Author to whom correspondence should be addressed. e-mail: piezolab@hfut.edu.cn

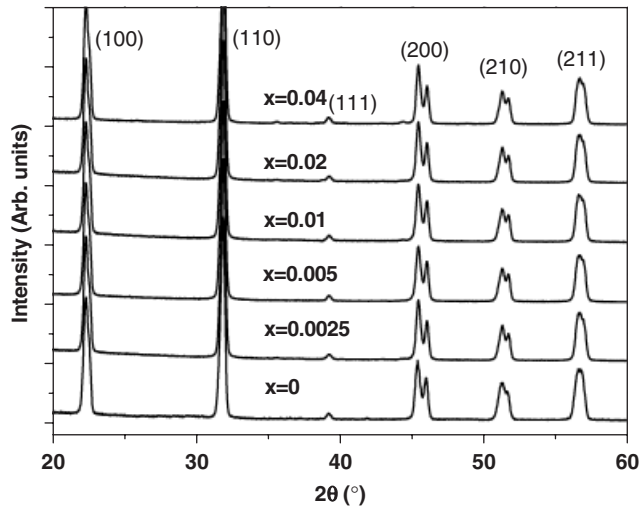


Fig. 1. X-ray diffraction patterns of $(\text{Na}_{0.5}\text{K}_{0.5})_{0.96}\text{Li}_{0.04}(\text{Ta}_{0.1}\text{Nb}_{0.9})_{1-x}\text{Cu}_x\text{O}_{3-3x/2}$ ceramics with different x as indicated.

erties at the frequency of 100 kHz were measured as a function of temperature by an LCR meter (HP 4284A, Hewlett-Packard, Palo Alto, CA). Polarization and strain hysteresis loops were measured in a silicone oil bath by applying an ac field at a frequency of 300 mHz by means of a modified Sawyer-Tower bridge. After a poling treatment in a silicone oil bath at 3 kV/mm for 20 min, the piezoelectric strain constant d_{33} and the

planar electromechanical coupling factor k_p were measured using a Belincourt-meter (YE2730, Sinocera, Shanghai, China) and a resonance-antiresonance method through an impedance analyzer (HP 4192A, Hewlett-Packard), respectively.

III. Results and Discussion

The effect of a small amount of CuO addition on the crystal structure of NKLTN ceramics is shown in Fig. 1. It can be seen that all compositions studied show pure perovskite structures with an orthorhombic symmetry. The CuO addition did not generate any second phases and evident lattice distortion. On the one hand, the formation of oxygen vacancies as a charge equilibrium mechanism tends to cause the lattice shrinkage. On the other hand, considering that Cu^{2+} has a relatively large ionic radius compared with Nb^{5+} (ionic radii: 0.73 and 0.64 Å for Cu^{2+} and Nb^{5+} , respectively, CN = 6),²³ lattice expansion can be expected by increasing the content of CuO. These two effects compensate with each other, leading to nonshift in the position of diffraction peaks. From Fig. 1(a) conclusion can also be drawn that Cu^{2+} has a solubility limit of more than 4% in the NKLTN perovskite lattice. There is doubt as to whether or not Cu^{2+} enters into the perovskite lattice of the matrix composition. In combination with other characterization techniques, this point can be made clearer in the following text.

Figure 2 shows the microstructure of NKLTN ceramics doped with different amounts of CuO sintered at 1080°C for 5 h. It should be noted that grains are significantly coarsened with doping CuO. The grain size is approximately 1.6 μm for pure

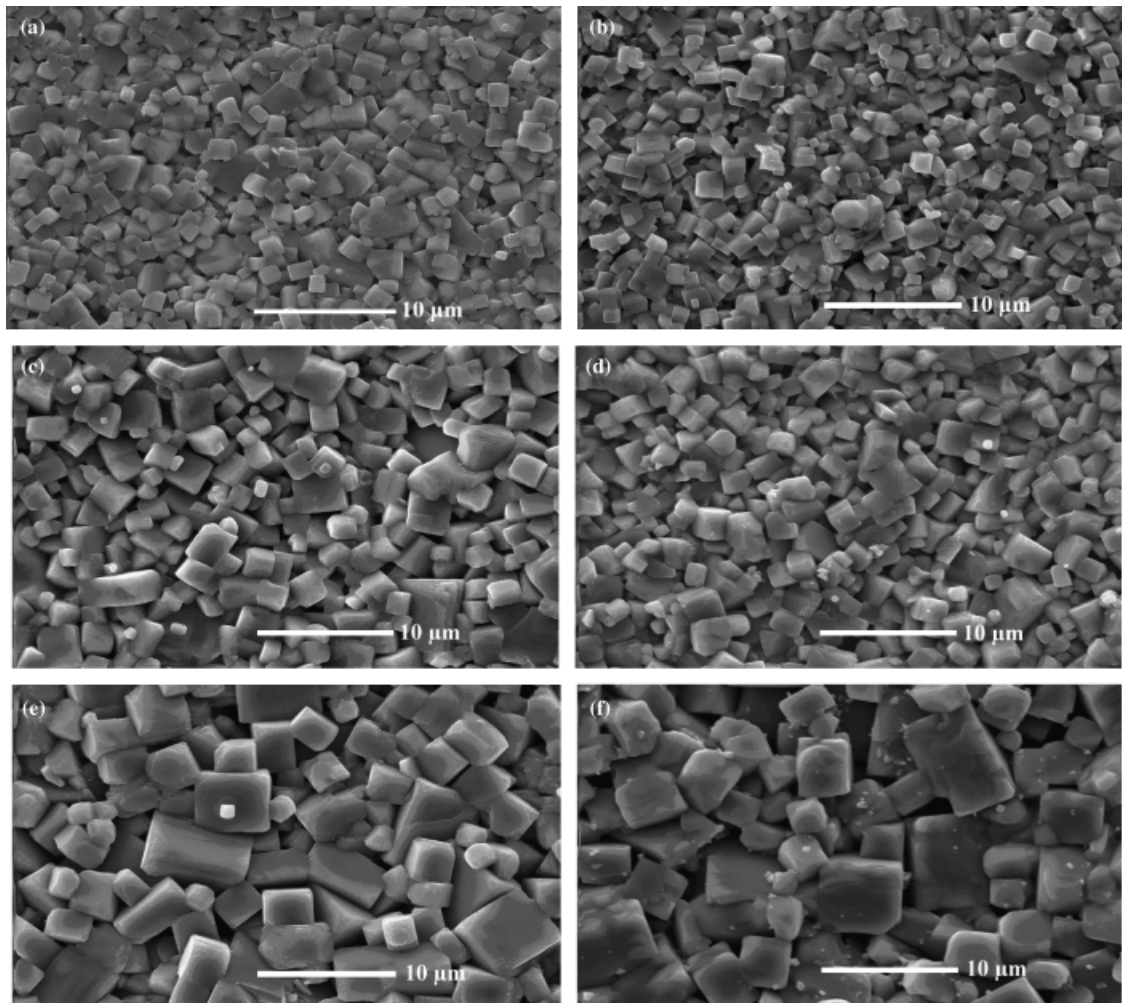


Fig. 2. Grain morphology of $(\text{Na}_{0.5}\text{K}_{0.5})_{0.96}\text{Li}_{0.04}(\text{Ta}_{0.1}\text{Nb}_{0.9})_{1-x}\text{Cu}_x\text{O}_{3-3x/2}$ ceramics with x equal to (a) 0, (b) 0.0025, (c) 0.005, (d) 0.01, (e) 0.02, and (f) 0.04.

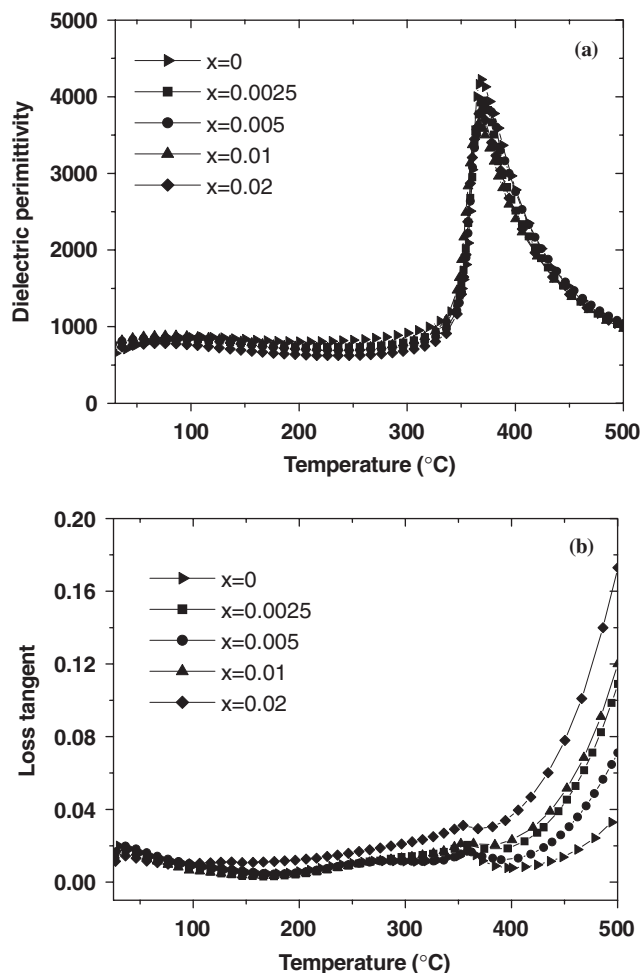


Fig. 3. Dielectric permittivity (a) and loss tangent (b) at 100 kHz of $(\text{Na}_{0.5}\text{K}_{0.5})_{0.96}\text{Li}_{0.04}(\text{Ta}_{0.1}\text{Nb}_{0.9})_{1-x}\text{Cu}_x\text{O}_{3-3x/2}$ ceramics with different x as indicated.

NKLTN, and increases to approximately $5\ \mu\text{m}$ for 1 mol% CuO-doped NKLTN. A significant grain growth in 4 mol% CuO-doped NKLTN ceramics causes a degraded densification as seen from Fig. 2(d), because the sintering potential is inversely proportional to the grain size. Therefore, a small amount of CuO addition could be advantageous for sintering NKLTN ceramics. It was considered that the influence of CuO addition on the grain morphology and densification of NKLTN ceramics is attributed to the formation of the oxygen vacancies and the eutectic solution at $\sim 1020^\circ\text{C}$ as seen in the $\text{CuO}-\text{Nb}_2\text{O}_5$ binary phase diagram.²⁴

The dielectric properties of NKLTN ceramics with different contents of CuO are shown in Fig. 3. On the one hand, the dielectric constants were not significantly influenced by the CuO addition. Particularly, the two phase transitions, corresponding to an orthorhombic–tetragonal transition near room temperature and a tetragonal–cubic transition at the Curie point (T_c), respectively, were not shifted. This is probably correlated to the unchanged crystal symmetries after doping CuO. The discrepancy in the final densities contributes to slightly different dielectric maxima. On the other hand, the loss tangents changed to some extent due to the addition of CuO. At lower temperature, the change of the loss tangent is not considerable. However, with increasing temperature, the difference in loss tangents of different samples becomes bigger. By comparison, when the doping level of CuO is $<1\%$, the difference in loss tangents is still not considerable in the temperature range of room temperature to $\sim 350^\circ\text{C}$. At the high-temperature region above 400°C , the loss tangent clearly increases with doping CuO. Generally speaking, the formation of oxygen vacancies may induce hard properties

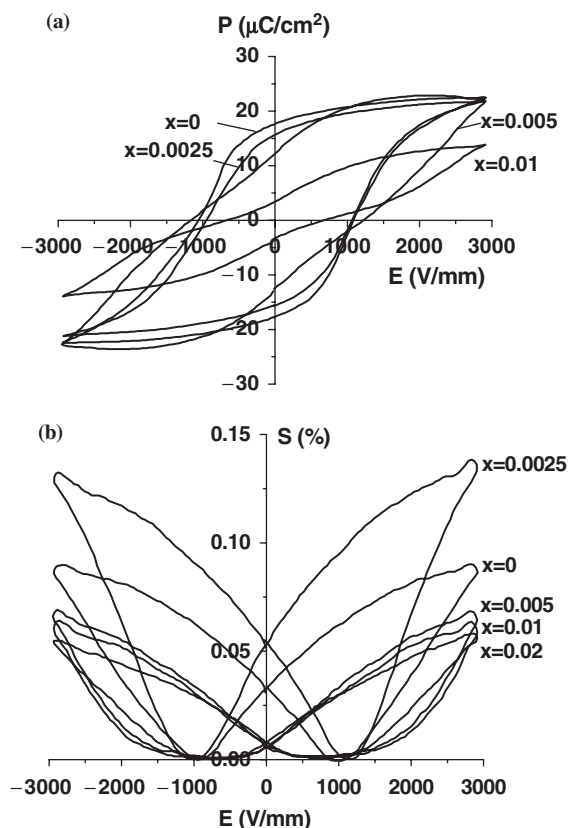


Fig. 4. Polarization (a) and strain (b) versus electric field loops for $(\text{Na}_{0.5}\text{K}_{0.5})_{0.96}\text{Li}_{0.04}(\text{Ta}_{0.1}\text{Nb}_{0.9})_{1-x}\text{Cu}_x\text{O}_{3-3x/2}$ ceramics with different x as indicated.

in the materials. Therefore, the loss tangent should decrease to some extent. In our study, the loss tangent increases at a higher doping level of CuO, probably due to that Cu exhibits two different charge states (Cu^{2+} and Cu^{1+}) controlled by the sintering atmosphere and the sintering parameters.²⁵

Figure 4 shows hysteresis loops of polarization and strain versus electric fields for CuO-doped NKLTN ceramics. The loops changed dramatically with increasing CuO content. Pure NKLTN ceramics have a remanent polarization P_r of $17.6\ \mu\text{C}/\text{cm}^2$ and a coercive field E_c of $1.1\ \text{kv}/\text{mm}$. When 0.25% CuO is added, both P_r and E_c of NKLTN ceramics slightly change, but strain values significantly increase. When the doping level of CuO increases up to 0.5%, E_c considerably increases and the ceramics exhibit a characteristic of hard materials, as clearly seen from the shape of the P – E loops. At the same time, the electric field-driven strains S get down. The hard feature in perovskite piezoelectric ceramics is usually attributed to oxygen vacancies. The replacement of Cu^{2+} for Nb^{5+} at the B site in the perovskite lattice of NKLTN ceramics produces oxygen vacancies for the charge equilibrium. The increase in S due to a small amount of CuO (0.25%) may come from the improvement of the sintering behavior probably involving grain size and morphology, and electrical resistivity, etc., as discussed above.

The various piezoelectric and electromechanical properties of CuO-doped NKLTN ceramics are listed in Table I. All samples have up to 96% of theoretical densities, except for 4% CuO-doped compositions where considerable grain growth occurred. The more than 1% CuO-doped NKLTN ceramics have increased loss tangents, leading to difficulty in the measurement of the P – E loop and the poling treatment. The promotion of densification due to the addition of 0.25% CuO causes the increase of the piezoelectric constant d_{33} and the planar electromechanical coupling factor k_p . On the contrary, when more than 0.25% CuO is doped, the hardened piezoelectric compositions exhibit decreased d_{33} and k_p . Both d_{33} and k_p decrease when the CuO

Table I. Room-Temperature Dielectric and Piezoelectric Properties of $(\text{Na}_{0.5}\text{K}_{0.5})_{0.96}\text{Li}_{0.04}(\text{Ta}_{0.1}\text{Nb}_{0.9})_{1-x}\text{Cu}_x\text{O}_{3-3x/2}$ Ceramics

CuO content, 100 ×	0	0.25	0.5	1	2	4
Relative density (%)	96	98	98	97	96	95
Dielectric permittivity at 25°C, 100 kHz	634	706	764	787	697	650
Loss tangent, at 25°C, 100 kHz	0.018	0.017	0.019	0.02	0.045	0.09
Piezoelectric constant, d_{33} (pC/N)	160	198	170	120	80	70
Coupling factor k_p (%)	43	45	42	41	38	35

CuO, copper oxide.

content increases to 1 mol%, although the density does not clearly change. Of course, when the doping level is higher, the decrease in density also contributes to the reduction of piezoelectric properties. The coexistence of two charge states of Cu ions after sintering causes the loss tangent (the electrical conductivity) to increase when more than 1% CuO is added. Therefore, the influence of CuO addition on NKLTN piezoelectric ceramics proves to be advantageous only when a small amount (<1%) is applied. Hard properties can be induced as the quantity of CuO increases.

IV. Conclusions

Lead-free NKLTN piezoelectric ceramics doped with CuO were manufactured using the conventional mixed-oxide route. It was found that CuO exhibits a significant influence on the densification and microstructure of NKLTN ceramics. The dielectric constants and phase transitions were not considerably changed by the addition of CuO. The loss tangents increase when the doping level increases, probably due to the coexistence of Cu^{2+} and Cu^{1+} . A small amount of CuO tends to increase the piezoelectric properties of NKLTN ceramics based on promoted densification; however, more CuO addition makes the materials become hard as an acceptor dopant.

References

- ¹R. Guo, L. E. Cross, S. E. Park, B. Noheda, D. E. Cox, and G. Shirane, "Origin of the High Piezoelectric Response in $\text{PbZr}_{1-x}\text{Ti}_x\text{O}_3$," *Phys. Rev. Lett.*, **84** [23] 5423–6 (2000).
- ²H. Fu and R. E. Cohen, "Polarization Rotation Mechanism for Ultrahigh Electromechanical Response in Single Crystal Piezoelectrics," *Nature*, **403**, 281–3 (2000).
- ³H. Cao, J. F. Li, and D. Viehland, "Electric-Field-Induced Orthorhombic to Monoclinic M–B Phase Transition in [111] Electric Field Cooled $\text{Pb}(\text{Mg}_{1/3}\text{Nb}_{2/3})\text{O}_3$ –30% PbTiO_3 Crystals," *J. Appl. Phys.*, **100** [8] 084102 (2006).
- ⁴T. Takenaka, K. Maruyama, and K. Sakata, " $(\text{Bi}_{0.5}\text{Na}_{0.5})\text{TiO}_3$ – BaTiO_3 System for Lead Free Piezoelectric Ceramics," *Jpn. J. Appl. Phys.*, **30** [9B] 2236–9 (1991).
- ⁵H. Nagata and T. Takenaka, "Lead Free Piezoelectric Ceramics of $(\text{Na}_{0.5}\text{Bi}_{0.5})\text{TiO}_3$ –1/2 $(\text{Bi}_2\text{O}_3\text{Sc}_2\text{O}_3)$ System," *Jpn. J. Appl. Phys.*, **36** [9B, Part 1] 6055–7 (1997).
- ⁶A. Sasaki, T. Chiba, Y. Mamiya, and E. Otsuki, "Dielectric and Piezoelectric Properties of $(\text{Bi}_{0.5}\text{Na}_{0.5})\text{TiO}_3$ – $(\text{Bi}_{0.5}\text{K}_{0.5})\text{TiO}_3$ Systems," *Jpn. J. Appl. Phys.*, **38**, 5564–7 (1999).

⁷T. Wada, K. Toyoiike, Y. Imanaka, and Y. Matsuo, "Dielectric and Piezoelectric Properties of $(\text{A}_{0.5}\text{Bi}_{0.5})\text{TiO}_3$ – ANbO_3 (A = Na, K) Systems," *Jpn. J. Appl. Phys.*, **40**, 5703–5 (2001).

⁸D. Q. Xiao, D. M. Lin, J. G. Zhu, and P. Yu, "Investigation on the Design and Synthesis of New Systems of BNT-Based Lead-Free Piezoelectric Ceramics," *J. Electroceram.*, **16**, 271–5 (2006).

⁹Y. Saito, H. Takao, I. Tani, T. Nonoyama, K. Takatori, T. Homma, T. Nagaya, and M. Nakamura, "Lead-Free Piezoceramics," *Nature*, **432**, 84–7 (2004).

¹⁰Y. Guo, K. I. Kakimoto, and H. Ohsato, "Phase Transitional Behavior and Piezoelectric Properties of $(\text{Na}_{0.5}\text{K}_{0.5})\text{NbO}_3$ – LiNbO_3 Ceramics," *Appl. Phys. Lett.*, **85**, 4121–3 (2004).

¹¹E. Hollenstein, M. Davis, D. Damjanovic, and N. Setter, "Piezoelectric Properties of Li- and Ta-Modified $(\text{Na}_{0.5}\text{K}_{0.5})\text{NbO}_3$ Ceramics," *Appl. Phys. Lett.*, **87**, 182905 (2005).

¹²S. J. Zhang, R. Xia, T. R. ShROUT, G. Z. Zang, and J. F. Wang, "Piezoelectric Properties in Perovskite $0.948\text{K}_{0.5}\text{Na}_{0.5}\text{NbO}_3$ – 0.052LiSbO_3 Lead-Free Ceramics," *J. Appl. Phys.*, **100**, 104108 (2006).

¹³R. Z. Zuo, X. S. Fang, and C. Ye, "Phase Structures and Electrical Properties of New Lead Free $(\text{Na}_{0.5}\text{K}_{0.5})\text{NbO}_3$ – $(\text{Bi}_{0.5}\text{Na}_{0.5})\text{TiO}_3$ Ceramics," *Appl. Phys. Lett.*, **90**, 092904 (2007).

¹⁴J. Yoo, K. Lee, K. Chung, S. Lee, K. Kim, J. Hong, S. Ryu, and C. Lhee, "Piezoelectric and Dielectric Properties of $(\text{LiNaK})(\text{NbTaSb})\text{O}_3$ Ceramics with Variation in Poling Temperature," *Jpn. J. Appl. Phys.*, **45** [9B] 7444–8 (2006).

¹⁵R. R. Zeyfang, R. M. Henson, and W. J. Maier, "Temperature- and Time-Dependent Properties of Polycrystalline $(\text{Li,Na})\text{NbO}_3$ Solid Solutions," *J. Appl. Phys.*, **48**, 3014–7 (1977).

¹⁶B. Malic, J. Bernard, J. Holc, D. Jenko, and M. Kosec, "Alkaline-Earth Doping in $(\text{K,Na})\text{NbO}_3$ Based Piezoceramics," *J. Eur. Ceram. Soc.*, **25**, 2707–11 (2005).

¹⁷S. H. Park, C. W. Ahn, S. Nahm, and J. S. Song, "Microstructure and Piezoelectric Properties of ZnO-Added $(\text{Na}_{0.5}\text{K}_{0.5})\text{NbO}_3$ Ceramics," *Jpn. J. Appl. Phys.*, **43** [8B] L1072–4 (2004).

¹⁸M. Matsubara, T. Yamaguchi, W. Sakamoto, K. Kikuta, T. Yogo, and S. I. Hirano, "Processing and Piezoelectric Properties of Lead-Free $(\text{K,Na})(\text{Nb,Ta})\text{O}_3$ Ceramics," *J. Am. Ceram. Soc.*, **88**, 1190–6 (2005).

¹⁹R. Z. Zuo, J. Rodel, R. Z. Chen, and L. T. Li, "Sintering and Electrical Properties of Lead-Free $\text{Na}_{0.5}\text{K}_{0.5}\text{NbO}_3$ Piezoelectric Ceramics," *J. Am. Ceram. Soc.*, **89** [6] 2010–5 (2006).

²⁰Y. Nakashima, W. Sakamoto, H. Maiwa, T. Shirura, and T. Yogo, "Lead Free Piezoelectric $(\text{K,Na})\text{NbO}_3$ Thin Films Derived from Metal Alkoxide Precursors," *Jpn. J. Appl. Phys.*, **46** [12–16] L311–3 (2007).

²¹J. Ryu, J. J. Choi, R. D. Hahn, D. S. Park, W. H. Yoon, and K. H. Kim, "Fabrication and Ferroelectric Properties of Highly Dense Lead Free Piezoelectric $(\text{K}_{0.5}\text{Na}_{0.5})\text{NbO}_3$ Thick Films by Aerosol Deposition," *Appl. Phys. Lett.*, **90** [15] 152901 (2007).

²²K. Chen, G. S. Xu, D. F. Yang, X. F. Wang, and J. B. Li, "Dielectric and Piezoelectric Properties of Lead Free $0.95(\text{K}_{0.5}\text{Na}_{0.5})\text{NbO}_3$ – 0.05LiNbO_3 Crystals Grown by the Bridgman Method," *J. Appl. Phys.*, **101** [4] 044103 (2007).

²³R. D. Shannon, "Revised Effective Ionic Radii and Systematic Studies of Interatomic Distances in Halides and Chalcogenides," *Acta Cryst.*, **A32**, 751–67 (1976).

²⁴V. P. Sirotnikin and N. M. Drozdova, "Interaction in Binary System of CuO – Nb_2O_5 ," *Russ. J. Inorg. Chem.*, **37** [11] 1334–6 (1992) (English Translation).

²⁵S. Priya, C. W. Ahn, and S. Nahm, "Dielectric Properties of $(\text{Ba}_{0.5}\text{Sr}_{0.5})(\text{Cu}_{1/3}\text{Nb}_{2/3})\text{O}_3$ System," *Ferroelectrics*, **322**, 75–82 (2005). □